



Silica-Shelled Cu-ZrO₂ Catalysts with Ultra-High Dispersion and Acidity for CO₂ Hydrogenation into Methanol and DME

Hebert D. P. Souza^{1*}, Vitor D. Lage¹, Fabio S. Toniolo^{1*}, Martin Schmal¹

¹Programa de Engenharia Química, Universidade Federal do Rio de Janeiro (UFRJ), NUCAT-COPPE, 21941-914 Rio de Janeiro/RJ, Brasil.

*hebert.int@gmail.com; * Toniolo@peq.coppe.ufrj.br

Resumo/Abstract

RESUMO – A hidrogenação de CO₂ em metanol e dimetil éter (DME) é uma rota promissora para a produção de combustíveis sustentáveis e compostos da química fina. Em catalisadores à base de cobre, a taxa de conversão de CO₂ também depende da área metálica de Cu, enquanto a seletividade à metanol e DME está ligada à razão Cu⁰/Cu⁺ e a acidez do catalisador, respectivamente. Neste trabalho, reportamos as propriedades e o desempenho catalítico dos catalisadores core-shell Cu-ZrO₂@SiO₂. Os materiais apresentaram alta área específica (> 400 m².g⁻¹), dispersão (14 – 60%) e área metálica de cobre (90 - 375 m².g⁻¹), e uma notável combinação de acidez de Brønsted e Lewis (> 780 μmol.g⁻¹). O catalisador Cu-ZrO₂@SiO₂ (3:2) alcançou seletividade acima de 70% para metanol, 8% em DME, conversão máxima de 28% e estabilidade acima de 72 horas. O XPS revelou a coexistência de espécies de cobre (Cu⁰/Cu⁺ e Cu²⁺) e ligação com a sílica (Cu²⁺–O– Si/ Cu⁺–O– Si), o que aumentou os sítios ativos disponíveis para a reação. A presença de espécies ZrO^{δ+} (ZrO_x e Zr –O– Si) e a alta concentração de defeitos estruturais também contribuiu para a adsorção de CO₂ e estabilidade das espécies de Cu, suprimindo a desativação oxidativa.

Palavras-chave: Hidrogenação de CO₂, síntese de metanol e DME, core-shell, cobre e zircônia, acidez de Brønsted e Lewis.

ABSTRACT – The catalytic hydrogenation of CO_2 to methanol and DME represents a viable pathway for sustainable fuel and fine chemical production. In Cu-based systems, CO_2 conversion strongly depends on the Cu metallic area, whereas methanol and DME selectivities are governed by Cu^0/Cu^+ ratio and catalyst acidity, respectively. Herein, we report the structural and catalytic features of core-shell $Cu-ZrO_2@SiO_2$ catalysts. The materials exhibited a high specific area (> 400 m².g¹¹), Cu dispersion (14 – 60%), and metallic area (90 – 375 m².g¹¹), and a remarkably dual Brønsted-Lewis acidity (> 780 m².g¹¹). The $Cu-ZrO_2@SiO_2$ (3:2) catalyst reached a selectivity up to 70% methanol, 8% DME, a maximum conversion of 28%, and stability over 72 h. XPS revealed a coexistence of $Cu^0/Cu^+/Cu^{2+}$ species and silica linkages ($Cu^{2+}-O-Si/Cu^+-O-Si$), enhancing the availability of active sites for the reaction. The presence of $ZrO_0^{\delta+}$ (ZrO_x and Zr-O-Si) and abundant structural defects facilitated CO_2 adsorption and Cu stabilization during the response, suppressing oxidative deactivation.

Keywords: CO₂ hydrogenation, methanol and DME synthesis, core-shell, copper and zirconia, Brønsted and Lewis acidity.

Introduction

The hydrogenation of CO₂ into value-added chemicals and fuels is a cornerstone strategy for addressing climate change and advancing a sustainable energy transition [1]. In this context, methanol and DME are exciting products for promoting efficient carbon neutrality and economy since these compounds serve as versatile building blocks for creating a wide array of products, including plastics, fuels, cosmetics, and other essential materials. [2].

Cu-based catalysts are distinguished by their high activity and selectivity for methanol and DME synthesis via CO₂ hydrogenation, in which Cu⁰ and Cu⁺ species play pivotal roles [3]. Cu⁰ facilitates CO₂ activation and H₂ spillover, whilst Cu⁺ stabilizes key reaction intermediates (e.g., CH₃O) critical for methanol formation. However, Cu-based catalysts often deactivate by water or coke poisoning during reaction. Besides, sintering of Cu particles may occur during calcination or reduction steps due to its Low Tamman temperature (405°C) [4]. Furthermore, integrating ZrO₂ into Cu-based catalysts further improves performance by enhancing copper dispersion and generating oxygen vacancies, facilitating CO₂ adsorption and H₂O dissociation. Additionally, zirconia provides Brønsted-Lewis acidity that drives the methanol-to-DME dehydration pathway [5]. On the other hand, silica coating is often employed as a



structural and electronic promoter, improving electron transference and suppressing coke formation and water-induced deactivation [3]. In this sense, this study explores the structural and catalytic features of core-shell Cu-ZrO₂@SiO₂ systems, highlighting their synergistic behaviour in CO_2 hydrogenation to methanol and DME.

Experimental

Synthesis of Core-shell catalysts

Cu-ZrO₂@SiO₂ catalysts were prepared by combining the reverse-micelle and modified Stöbber methods. First, an oily phase (n-dodecane, n-hexanol, and CTAB) was mixed with an aqueous phase of Cu and Zr nitrates with desired amounts of 10 wt. %. and 3.3 wt. %., respectively, under stirring and stabilized for a few hours to create micelle cores with metals. Then, the *in-situ* silica shell was created by adding a certain amount of TEOS dropwise, followed by ammonia hydroxide (28% v/v). The catalyst was washed, dried at 100°C, and calcined at 400°C. Different Cu:Zr ratios (1:0, 3:2, 3:3, and 0:1) were also prepared using this method.

Catalyst characterization

TEM analysis determined catalyst morphology, while the ICP-OES technique provided chemical composition. Textural properties were obtained by N_2 adsorption and desorption at 77 K. The surface species and their behaviour under a reductive environment were determined by NAP-XPS, whilst reducibility was evaluated by TPR analysis. Cu dispersion and metallic area were obtained by N_2 O chemisorption, and the catalyst acidity and basicity by N_3 -and CO_2 -TPD, respectively.

Catalytic tests

Catalytic performance was evaluated in a fixed-bed continuous-flow reactor loaded with 300 mg of catalyst diluted with inert SiO₂. Before the reaction, the catalyst was purged under helium at 150 °C for 30 minutes to remove impurities, followed by an *in-situ* reduction at 400 °C for 2 hours. After reduction, the system was cooled to 220 °C to initiate the reaction: 220 to 310 °C, pressure of 30 bar, space velocity of 6000 mg.mL⁻¹.h⁻¹, and a H₂/CO₂ molar ratio of 3. The feed gases (CO₂, H₂, and N₂) were controlled electronically. Gaseous products were analyzed online using a gas chromatograph.

Results and Discussion

Spherical morphology

The monometallic Cu@SiO₂ catalyst exhibited interconnected spheres with different sizes (Figure 1). The STEM-HAADF analysis was used to identify the presence of Cu atoms based on their Z-contrast, showcasing tiny



black dots. Additionally, the EDX elemental mapping confirmed the presence of copper by showing shiny teal-coloured dots and that Cu nanoparticles are homogeneously dispersed into the silica matrix, represented by purple dots. This suggests copper may be encapsulated in multicore and formed Cu–O–Si units by strongly interacting with silica.

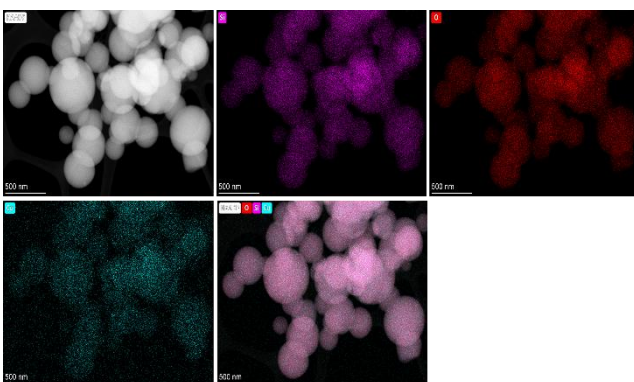


Figure 1. TEM

micrographs and STEM-EDX elemental mapping of $Cu@SiO_2$ catalyst. Colored dots: Si (purple), O (red), Cu (teal), and all elements (pink).

Under slightly basic medium (pH = 9), silanol groups (-OH) from silica are more likely to deprotonate and form siloxide anions (SiO⁻), and can strongly interact with Cu²⁺ and Cu⁺ species (eqs. 1 and 2) via the oxygen lone pair or siloxane bridges (Si–O–Si bonds) [3], described as follows:

$$Cu^{2+}_{(aq)} + 2Si-OH_{(\overline{aq})} \rightarrow (Si-O)_2-Cu_{(aq)} + 2H^{+}_{(aq)}$$
 (1)

$$Cu^{+}_{(aq)} + Si-OH_{(aq)} \longrightarrow (Si-O-Cu_{(aq)} + H^{+}_{(aq)})$$
 (2)

The existence of different copper-silica linkages (Cu²⁺-O- Si/ Cu⁺-O- Si) can be rationalized through molecular orbital theory (MOT) and ligand field theory (LFT). In aqueous environment, Cu2+ ions typically adopt an octahedral geometry as part of $[Cu(H_2O)_6]^{2+}$ aqua complex [6,7], where the approach of ligands (H₂O) induces a crystal field splitting of the 3d orbitals into two sets: the higher energy eg orbitals (dz2 and dx2-v2) and the lower energy t2g orbitals (dxy, dxz, and dyz). Uneven occupancy of eg orbital, characterized by a single unpaired electron in the dz2 orbital and two in the dx2-y2 orbital, results in an anisotropic electronic distribution. This instability drives a Jahn-Teller distortion, typically manifesting as an axial elongation of Cu-O bonds (along the z-axis) and a concomitant compression in the equatorial plane (xy planes of dx2-y2 orbital), effectively lowering the system's energy by relieving degeneracy-induced repulsion.

This distortion promotes orbital overlap between the Cu 3d orbitals and the O 2p orbitals of surface silanol groups (–



OH), facilitating the formation of Cu²⁺–O–Si linkages. In contrast, Cu⁺ ions, characterized by a filled 3d shell and vacant 4s orbital, engage in σ-type coordination with silanol groups via ligand-to-metal donation. The resulting Cu⁺–O–Si interactions are stabilized through back-donation mechanisms, wherein lone pair electrons from oxygen are donated into the empty 4s orbital of Cu⁺, reinforcing the covalent character of the bond. These Cu–O–Si units act as sites during CO₂ hydrogenation [3].

Stabilized Cu⁰ and Cu⁺ redox pair by zirconia and silica

NAP-XPS revealed the coexistence of different Cu oxidation states (Cu⁰/Cu⁺, and Cu²⁺) and Cu-O-Si units (Figure 2). Under analysis conditions, RT-UHV, Cu 2p orbital exhibited four peaks (black line spectra). The main peaks are attributed to Cu 2p_{3/2} (933.6 – 935.3 eV) and Cu $2p_{1/2}$ (948.1 – 959.8 eV) orbitals, with a spin-orbit coupling (SOC) of 20.8 eV. Satellite peaks are exhibited at 943.3 eV and 952.8 eV and indicate the presence of the CuO phase. The deconvolution of Cu 2p_{3/2} showed two components at 933.2 and 935.7 eV, assigned to the $Cu^{\delta+}$ (0 < δ < 2), a mixed valence oxidation state related to Cu²⁺-O-Si units, and Cu²⁺ species, respectively [3,8]. The same was observed in the region of 2p_{1/2} with peaks at 953.1 eV and 955.5 eV, associated with Cu⁺-O-Si units and Cu⁰/Cu⁺ species, respectively. In addition, under 2 mbar and H₂ atmosphere, as the temperature increases, the Cu 2p satellite peaks gradually disappear, and the intensity of components on Cu $2p_{3/2}$ and Cu $2p_{1/2}$ located at 935.7 eV and 955.7 eV, respectively, is diminished. These results suggest that Cu²⁺ and Cu⁺ species on the surface undergo reduction.

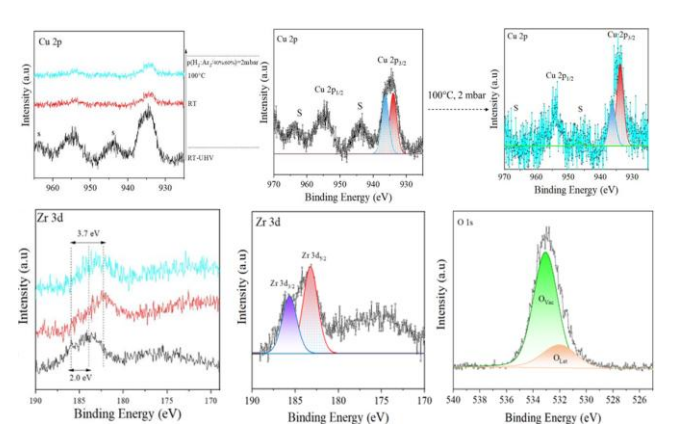


Figure 2. XPS spectra of Cu-ZrO₂@SiO₂ (3:1) catalyst obtained from room temperature to 100°C at 2 mbar, and deconvoluted RT-UHV spectra of Cu 2p, Si 2p, and Zr 3d orbitals.

The XPS spectra of Zr 3d showed a characteristic spinorbit doublet at 183.2 eV and 185.8 eV with a SOC energy of 2.4 eV, consistent with Zr⁴⁺ species and Zr–O bonding environments [14]. Notably, these values are positively



shifted compared to those typically reported for stoichiometric ZrO_2 . This suggests that the emergence of $Zr^{\delta+}$ species – intermediate in oxidation state between Zr^{3+} and Zr^{4+} – indicates a more covalent Zr–O interaction [9]. This electronic perturbation is further corroborated by the deconvolution of O1s spectra, which exhibits a pronounced component at 533.0 eV, corresponding to oxygen associated with structural defects or near vacancies (O_{Vac}). In contrast, the oxygen in the lattice (O_{Lat}) has a small contribution at 532.0 eV. The O_{Vac}/O_{Lat} ratio of 4.20 confirms a substantial concentration of oxygen defects, likely induced during the synthesis and calcination step, and underscores the defectrich nature of the catalyst.

Such structural and electronic modifications were also reflected in the redox behavior of the catalysts. TPR profiles (Figure 3) demonstrated an increase in the reduction temperature of Cu species upon incorporation of ZrO2, particularly in catalysts with higher zirconia loading. For instance, the extent of Cu reduction decreased from 51% in the monometallic system to 43% in the Cu-ZrO₂@SiO₂ (3:3) bimetallic catalyst, indicating the stabilization of Cu species. Interestingly, this behavior contrasts with a previous report by Liu et al. [10], where ZrO₂ promoted the reduction of Ni species in Ni-ZrO₂@SiO₂ catalyst relative to Ni@SiO2 and Ni-ZrO2/SiO2. However, our findings are consistent with the trends reported by Wang et al., [11], who reported a sequential downshift in the main Cu reduction peak in the order Cu/ZrO₂-SiO₂ < Cu/ZrO₂ < Cu/SiO₂. These observations suggest a strong Cu-Zr interaction mediated by the synthesis method, which is critical in modulating the reducibility and dispersion of Cu species within the silica matrix.

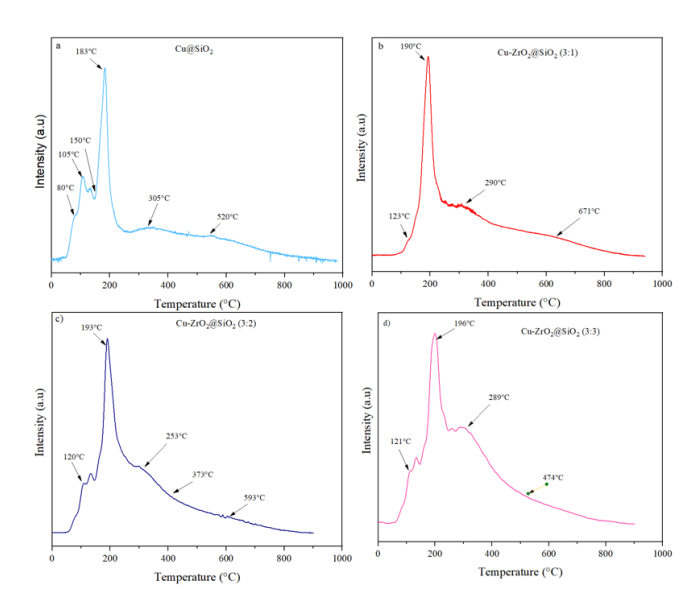


Figure 3. TPR profiles of monometallic $Cu@SiO_2$ and bimetallic $Cu-ZrO_2@SiO_2$ catalysts.



Finally, above 500°C, the width of H₂-TPR profiles may suggest the presence of multiple reducible species with varying chemical environments and degrees of interaction, for instance Cu²⁺ species strongly interacting with ZrO₂ or embedded with SiO₂ domains. In addition, progressive dehydroxylation of surface silanol groups (Si – OH) to form siloxane bridges (Si–O–Si) may also occur [12,13] with concomitant release of H₂O. The partial dehydroxylation of silica may lead to a less hydrophilic surface, thereby decreasing water adsorption, the by-product of CO₂ hydrogenation, and mitigating the deactivation phenomena related to oxidation of Cu species or sintering.

Tailored textural properties enabled by core-shell design

The Cu-ZrO₂@SiO₂ catalysts exhibited a remarkably high surface area of over 400 m².g⁻¹, significantly greater than traditional Cu-based catalysts for synthesizing methanol and DME. This enhancement stems from a synthesis strategy that improved the dispersion of ZrO₂, which enhanced the dispersion of Cu. The presence of Zr⁴⁺ species also confers a greater positive charge density, acts as an effective structural modifier of the silica matrix, and may form stable pores and interfaces [14]. On the other hand, the silica encapsulation prevents the pores from collapsing during calcination and preserves a mesoporous structure favorable for reactant diffusion. Table 1 presents the textural properties evaluated through N₂ physisorption.

Table 1. Textural properties of monometallic and bimetallic Cu-ZrO₂@SiO₂ catalysts measured by N_2 physisorption

Catalyst	S_{BJH}	PV	PD
	$(m^2.g^{-1})$	$(cm^3.g^{-1})$	(nm)
Cu-ZrO ₂ @SiO ₂ (3:3)	563	0.43	3
Cu-ZrO ₂ @SiO ₂ (3:2)	534	0.63	5
Cu-ZrO ₂ @SiO ₂ (3:1)	418	0.85	8
$ZrO_2@SiO_2$	437	0.93	8
Cu@SiO ₂	10	0.02	15
10% Cu-ZrO ₂	87	0.07	3

PV = Pore volume; PD = Pore diameter

Zirconia enhanced Cu dispersion and metallic surface area

The Cu@SiO₂ catalyst displayed a dispersion (D_{Cu}) of 14% and 91 m².g⁻¹ of metallic area (S_{Cu}). These values are also significantly higher than the reference 10%Cu/ZrO₂ catalyst, which showed poor copper dispersion (5%) and metallic area (33 m².g⁻¹), as observed in Table 2. The bimetallic Cu-ZrO₂@SiO₂ (3:1) catalyst containing 10% wt. of Cu and 3.3% wt. of ZrO₂ showed the highest dispersion (57%) and metallic area (374 m².g⁻¹), with the most minor Cu particle diameter (1.7 nm), followed by ZrO₂@SiO₂



(3:2). Interestingly, the Cu-ZrO₂@SiO₂ (3:3) with the highest specific area (563 m².g¹¹) exhibited similar values D_{Cu} (14%) and S_{Cu} (93 m².g¹¹) of Cu@SiO₂ catalyst. This result may suggest that higher ZrO₂ content (10% wt.) may partially block the mesoporous silica network or promote aggregation of ZrO₂ domains, reducing the number of accessible anchoring sites for Cu and favoring the growth of larger Cu particles. Another hypothesis is a phase segregation that reduces the synergistic Cu–Zr interactions crucial for stabilizing small Cu nanoparticles.

 $\begin{tabular}{ll} \textbf{Table 2.} & Physicochemical properties of Cu-based core-shell \\ catalysts measured by N_2O chemisorption \\ \end{tabular}$

Catalyst	Dispersion	Metallic area	d_{Cu}	
Cataryst	(%)	$(m^2.g^{-1})$	(nm)	
Cu-ZrO ₂ @SiO ₂	14	93	7	
(3:3)	14	93	,	
Cu-ZrO ₂ @SiO ₂	34	224	3	
(3:2)	34	224	3	
Cu-ZrO ₂ @SiO ₂	57	374	2	
(3:1)	37	371		
Cu@SiO ₂	14	95	7	
10%Cu-ZrO ₂	5	33	22	

Acidity of ZrO₂ drives methanol dehydration to DME

NH₃-TPD (Table 3) revealed the presence of high-density Brønsted-Lewis acidity up to 760 μ mol.g⁻¹ for bimetallic catalysts, attributed primarily to zirconia, consisting of weak and moderate acid sites, essential to secondary methanol dehydration into DME. The weak Lewis acid sites of ZrO₂ consist of coordinately unsaturated Zr⁴⁺ ions (cus Zr⁴⁺) and cus O²⁻ act as basic centers to form acid-base pairs, whereas the Brønsted sites are amphoteric and correspond to hydroxyl groups (-OH) [15].

 $\begin{tabular}{ll} \textbf{Table 3.} & Physicochemical properties of Cu-based core-shell \\ catalysts measured by N_2O chemisorption \\ \end{tabular}$

Catalyst	NH ₃ desorption (μmol.g ⁻¹)	CO ₂ desorption (µmol.g ⁻¹)
Cu-ZrO ₂ @SiO ₂ (3:3)	1128	7
$\text{Cu-ZrO}_2 @ \text{SiO}_2$ (3:2)	1079	9
$\text{Cu-ZrO}_2 @ \text{SiO}_2$ (3:1)	768	10
Cu@SiO ₂	747	1
10%Cu-ZrO ₂	-	36



The surface basicity (Table 3) of mono- and bimetallic catalysts indicates poor CO₂ desorption (10 mol.g⁻¹), with the highest value obtained for the supported 10%Cu/ZrO₂ catalyst (36 mol.g⁻¹). This result agrees with those previously reported by Dang et al. [16], who observed a decrease in the basicity of SiO₂-ZrO₂ compared to the ZrO₂ catalyst, attributed to weak Brønsted sites formed at Zr–O–Si interfacial bonds.

High selectivity with competitive CO₂ conversion under mild conditions

The catalyst performance was evaluated based on temperature and time functions (Figure 4). Catalytic tests were performed at 220 - 310 °C, 30 bar, GSHV of 6000 mg.mL.h⁻¹, and H₂/CO₂ ratio of 3. At 220°C, the CO₂ conversion was 7% for Cu-ZrO₂@SiO₂ (3:2) catalyst with selectivities of 94.5% for methanol and 5.2% for DME. CO2 conversion, DME selectivity, and CO and CH4 are enhanced as the temperature increases. Under 280°C, the catalyst achieved nearly 20% CO2 conversion with methanol selectivity up to 80% and 9% DME, while the amount of CO and CH₄ remained 4% and 5%, respectively. These values compare favorably with more complex Cubased systems reported in the literature and demonstrate the efficacy of multifunctional core-shell design and the synthesis procedure. The high Cu metallic area enhanced hydrogen spillover and increased methanol production. Herein, this phenomenon refers to the dissociation of H₂ molecules at the metallic site of Cu particles and the migration of activated H atoms to the adjacent ZrO₂ particles, where protons (H⁺) diffuse to the O²⁻ anions to form O-H and H-O-H bonds and oxygen vacancies [17], and increased the selectivity toward the main products.

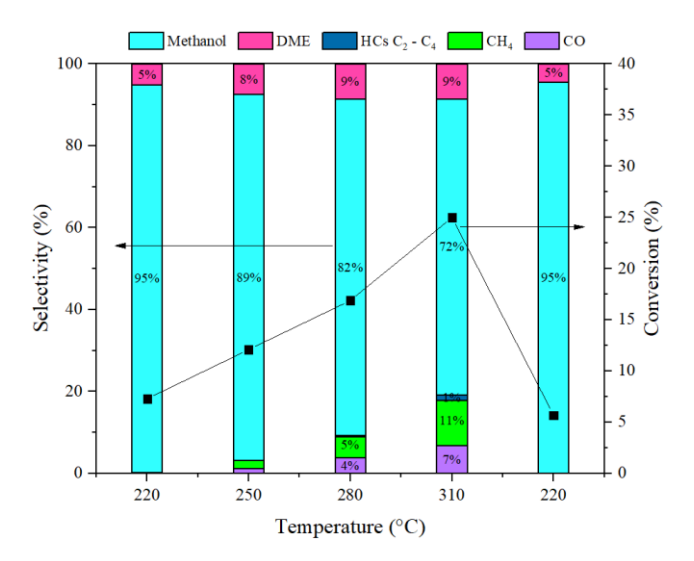


Figure 4. CO₂ conversion and DME selectivity increase with temperature.



The CO produced during all catalytic tests was lower than 10%, while CH₄ appeared at 250 °C (< 2%) and reached almost 11% at 310 °C. The presence of these by-products occurs due to competitive RWGS reaction and secondary hydrogenation that takes place as temperature increases and converts surface-adsorbed intermediates (e.g., HCO₂* \rightarrow H₂COH* \rightarrow CH₂* \rightarrow CH₃* \rightarrow CH₄* \rightarrow CH₄). It's worth mentioning that the catalyst remained stable for 72 h at 310°C and did not seem to deactivate, which can be observed by returning the catalyst to 220°C. The high selectivity and stability underscore the catalyst potential for deployment in industrial CO₂ hydrogenation processes focused on sustainable fuel production.

Conclusions

In this work, we developed and evaluated Cu-ZrO₂@SiO₂ core–shell catalysts for hydrogenating CO₂ to methanol and dimethyl ether (DME). The strategic integration of highly dispersed Cu nanoparticles with acidic zirconia and a protective silica shell resulted in a high-performance multifunctional catalytic system. The catalysts achieved a high specific surface area (> 400 m².g¹¹), a remarkable Cu⁰ surface area (> 200 m².g¹¹), and strong acidity (up to 1000 μ mol/g), supporting both methanol synthesis and its dehydration to DME.

Integrating ZrO_2 into the catalyst enhanced Cu dispersion and provided acidic sites, while the silica shell stabilized the active Cu^0/Cu^+ redox pair and prevented deactivation by sintering. Under reaction conditions representative of industrial methanol synthesis (280°C, 30 bar, 6000 GHSV), the catalyst delivered nearly 25% CO_2 conversion with high selectivity (70% methanol, 9% DME) at 310°C, and excellent stability over 72 hours of continuous operation.

These results demonstrate the potential of rationally engineered hybrid catalysts to overcome long-standing limitations in CO₂ valorization and contribute meaningfully to sustainable energy systems.

Acknowledgments

This study was financed in part by the Coordenação de Aperfeiçoamento de Pessoal de Nível Superior – Brasil (CAPES). The authors would also like to thank the Centro Brasileiro de Pesquisas Físicas (CBPF) for the NAP-XPS analysis.

References

- 1. Dong, X. et al. Appl. Catal., B. **2016**, 191, 8 17.
- To, A. et al. Journal of CO₂ Utilization, 2022, 66, 102261.
- 3. Yu, J. et al. ACS Catalysis, 2020, 10, 14694 14706.





- 4. Dong, X. et al. Chinese Journal of Catalysis, **2017**, 38, 717 725.
- 5. Gao P. et al. J Catal, 2013, 298, 51–60.
- 6. Zheng, X. G. et al. *Physica C.* **2001**, 357–360, 181–5.
- 7. Liu, M. et al. J. Hazard Mater., 2024, 461, 132658.
- 8. Ding, J. et al. Appl. Catal. B. 2017, 209, 530–42.
- 9. Yao, L. et al. J. Catal. **2019**, 372, 74 85.
- 10. Liu, W. et al. Journal of CO₂ Utilization, **2018**, 27, 297 307.
- 11. Wang, D. et al. Chemistry Europe, **2017**, 2, 4823 4829.
- Santos, J. H. Z. J. Mol. Catal. A Chem, 1999, 139, 199– 207.
- 13. Teles, C. A. Catalysis, **2016**, 146, 1848 1857.
- 14. Lu, X. et al. Npj Materials Degradation, 2018; 2, 19.
- 15. Viinikainen, T. *et al. Applied Catalysis A General*, **2009**, 362, 169 77.
- 16. Dang, Z. et al. J. Phys. Chem. 1995, 99, 14437-43.
- 17. Shen, H. *et al.* Green Energy & Environment, **2022**, 7, 1161 1198.